PROCEEDINGS OF
THE ROYAL SOCIETY B
BIOLOGICAL SCIENCES

Morphological convergence obscures functional diversity in sabre-toothed carnivores

Journal:	*Proceedings B*
Manuscript ID	RSPB-2020-1818.R1
Article Type:	Research
Date Submitted by the Author:	03-Sep-2020
Complete List of Authors:	Lautenschlager, Stephan; University of Birmingham, Figueirido, Borja; Universidad de Málaga Cashmore, Daniel; University of Birmingham Bendel, Eva-Maria; Museum für Naturkunde - Leibniz-Institut für Evolutions- und Biodiversitätsforschung; Humboldt-Universität zu Berlin Stubbs, Thomas; University of Bristol, School of Earth Sciences
Subject:	Palaeontology < BIOLOGY, Evolution < BIOLOGY
Keywords:	Convergent evolution, functional morphology, computational analysis, Smilodon, ecology
Proceedings B category:	Palaeobiology

Author-supplied statements

Relevant information will appear here if provided.

Ethics

Does your article include research that required ethical approval or permits?:
This article does not present research with ethical considerations

Statement (if applicable):
CUST_IF_YES_ETHICS :No data available.

Data

It is a condition of publication that data, code and materials supporting your paper are made publicly available. Does your paper present new data?:
Yes

Statement (if applicable):
All data files are available via the following link:
https://beardatashare.bham.ac.uk/getlink/fiR7wvK357hbPrQ9FVg6eR1Q/ Upon acceptance the files will be moved to a permanent repository (e.g. Dryad, Zenodo; depending on journal integration policy).

Conflict of interest

I/We declare we have no competing interests

Statement (if applicable):
CUST_STATE_CONFLICT :No data available.

Authors' contributions

This paper has multiple authors and our individual contributions were as below

Statement (if applicable):
S.L conceived the study and designed the analyses. S.L., D.D.C and T.L.S. conducted the analyses and designed the figures. B.F and E.-M.B. contributed to the datasets. All authors contributed to the writing of the manuscript

Morphological convergence obscures functional diversity in sabre-toothed carnivores

Stephan Lautenschlager[1], Borja Figueirido[2], Daniel D. Cashmore[1], Eva-Maria Bendel[3,4], Thomas L. Stubbs[5]

[1]School of Geography, Earth and Environmental Sciences, University of Birmingham, Edgbaston, Birmingham B15 2TT, UK
[2]Universidad de Málaga, Departamento de Ecología y Geología, Facultad de Ciencias, 29071-Málaga, Spain.
[3]Museum für Naturkunde, Leibniz-Institut für Evolutions- und Biodiversitätsforschung, Invalidenstraße 43 10115 Berlin, Germany
[4]Institut für Biologie, Humboldt-Universität zu Berlin, Invalidenstraße 42, 10115 Berlin, Germany
[5]School of Earth Sciences, University of Bristol, 24 Tyndall Avenue, Bristol BS8 1TQ, U.K.

The acquisition of elongated, sabre-like canines in multiple vertebrate clades during the last 265 million years represents a remarkable example for convergent evolution. Due to striking superficial similarities in the cranial skeleton, the same or similar skull and jaw functions have been inferred for sabre-toothed species and interpreted as an adaptation to subdue large-bodied prey. However, although some sabre-tooth lineages have been classified into different ecomorphs (dirk-tooths and scimitar-tooths) the functional diversity within and between groups and the evolutionary paths leading to these specialisations are unknown. Here, we use a suite of biomechanical simulations to analyse key functional parameters (mandibular gape angle, bending strength, bite force) to compare the functional performance of different groups and to quantify evolutionary rates across sabre-tooth vertebrates. Our results demonstrate a remarkably high functional diversity between sabre-tooth lineages and that cranial function and prey killing strategies evolved within clades. Moreover, different biomechanical adaptations in coexisting sabre-tooth species further suggest that this functional diversity was at least partially driven by niche-partitioning.

Key words: Convergent evolution, functional morphology, computational analysis, *Smilodon*, ecology

1. Introduction

The sabre-toothed cat *Smilodon fatalis* from the Pleistocene of North America represents one of the most iconic and instantly recognisable vertebrate fossils [1]. Its distinct morphology characterised by the eponymous, elongated canine teeth, has received considerable academic and public attention [2-4]. However, sabre-toothed species were much more diverse and widespread in the fossil record than the prominence of this single well-known species would suggest. Although only loosely defined and not equally distributed across different species, sabre-tooth morphologies, such as elongate and mediolaterally flattened canines, an often anteroposteriorly compressed braincase, and a reduced coronoid process, have evolved several times convergently: in metatherians (thylacosmilines), in eutherians (independently in creodonts, nimravids, barbourofelids, and machairodontine felids), and outside of Mammalia in Permian gorgonopsians [5,6] (figure 1).

Through time, sabre-toothed carnivores showed a near-global distribution across North America, Europe, Africa and Asia and dominated many terrestrial ecosystems during the Permian and the Cenozoic [1,7]. This repeated occurrence of sabre-toothed morphologies in different, and often unrelated, groups separated by up to 200 million years has been explained with independent adaptations for subduing large-bodied prey [5,8 although see 9]. Furthermore, the presence of sabre-toothed characters has been hypothesised to provide distinct functional advantages [10], which are thought to represent functional optimisation and trend towards increasingly specialized feeding/hunting adaptations in each lineage [11].

Several characters have been discussed as performance indicators in sabre-toothed taxa, including the evolution of a large jaw gape, decreased or increased bite forces and improved stability of the craniodental complex [4,12-14]. However, functional studies of sabre-toothed predators have often focused on single well-known or well-preserved species within each lineage, and these have usually been the most derived taxa impeding inferences about evolutionary trajectories [4,5,13]. This traditional focus on derived taxa has further led to the assumption of functional and evolutionary convergence across sabre-toothed forms. However, caution is warranted over simplified

morphological comparisons, as morphological convergence can be a poor indicator for functional convergence [15,16]. Nevertheless, similar ecomorphologies, prey selection, hunting and killing behaviour have been suggested for all sabre-tooths, although some functional differences between scimitar-toothed and dirk-toothed taxa have been recognised [5,6,14,17,18].

Here, we investigate the evolution of sabre-toothed morphologies across different clades and over the last 265 million years from a biomechanical perspective. We test the hypothesis that functional trends were decoupled and divergent from morphologically convergent trajectories. Specifically, we obtain biomechanical performance measures (jaw gape, mandibular stability, bite force), which have been demonstrated to correlate with known biologically and ecologically meaningful properties [19-21]. Using a combination of biomechanical modelling and phylogenetic comparative methods, we find that most of the sabre-tooth clades evolved towards different functional specialisations acquired via variable evolutionary pathways.

2. Material and methods

(a) Specimen selection

A total of 66 species were sampled from the literature and analysed (see supplementary material) (figures 1, S1*a*). Only taxa which preserved the complete craniomandibular skeleton were selected, as well as a few incomplete taxa, which could be reconstructed with minimal interpretation. This allowed for over 50% of established species and over 70% of established genera to be sampled in each group. Two-dimensional outlines of each specimen were generated using Adobe Illustrator CC (Adobe Inc.) (figure S1*b*) and muscle attachment sites of the masseter and the temporalis muscle groups were mapped onto the cranial outlines (the pterygoideus group was not considered due to its largely mediolateral line of action and negligible contribution to gape angle and bite force) for the mammalian taxa. For the gorgonopsian taxa, the m. adductor mandibulae externus (m. AME) complex, the pterygoideus muscles and the pseudotemporalis muscles were each considered as a single functional unit.

85

86 **(b) Gape analysis**

87 For the gape analysis, the images of the cranial outlines were imported into Blender
88 (www.blender.org, version 2.79) to generate simplified skull and jaw models (figure S1*c*) using a
89 box-modelling approach [22]. The outlines were extruded in the third dimension by a consistent
90 width of 2 mm (we refer to these simplified three-dimensional models as extruded models following
91 [23]).

92 The gape analysis (figures 2, S1*d*) followed the methodology detailed in [24]. The skull and
93 mandible models were joined at the jaw joint and the mandible was allowed full rotation around the
94 mediolateral axis (y-axis) to simulate sagittal opening and closing. Adductor muscles were
95 represented by cylinders connecting the attachment sites projected onto the extruded models. An
96 opening motion with a step size of 0.5 degrees was imposed on the lower jaw, during which the
97 muscle cylinders were stretched. For each step, the ratio between the resting length and the
98 extended length of the muscle cylinders was calculated until any of the muscle cylinders reached
99 the critical extension limit of 170%. This extension limit was based on experimentally derived
100 values for mammalian adductor muscles above which tetanic tension of muscles is no longer
101 possible [24]. Although it cannot be ruled out that the non-mammalian taxa in this study had a
102 different muscle architecture, the same extension limit was assumed for consistency.

103 To test whether the extruded models could faithfully reproduce realistic results, the
104 methodology was validated using three-dimensional models of fossil sabre-tooths (*Smilodon fatalis*,
105 *Homotherium serum*, *Yoshi garevskii, Inostrancevia alexandri*) and extant felids (*Panthera leo*,
106 *Hyena hyena*), which covered the range of observed cranial morphologies (see supplementary
107 material). To further account for uncertainties regarding the exact muscle attachment, five different
108 variations in muscle arrangement were tested for each model and the average gape angle was
109 calculated. To evaluate how much the extruded models underestimate gape angles, a correction

factor was calculated (see supplementary material, figures S2-4). The obtained correction factor of 2.0 was then applied to the results from the extruded models.

(c) Finite element analysis

To assess the biomechanical performance of the studied taxa, finite element analyses (FEA) were performed (S1*e*). In comparison with full 3D models, the extruded models may not capture the full biological signal. However, it has been demonstrated that meaningful, shape-related biomechanical performance measures can be obtained from extruded models [23,25-28]. Sensitivity tests were performed by comparing FEA results obtained from corresponding extruded and full 3D models for selected taxa (see supplementary material, figures S5, S6). Only the mandible morphology was considered for FEA, as it can be more accurately replicated in this simplified context. Furthermore, the mandible provides a more reliable signal for feeding performance compared to the skull, which underlies constraints due to compromising functions [21].

For FEA, the extruded models of the lower jaws were exported from Blender as .STL files and imported into HyperMesh (Altair, version 11) for solid meshing and the setting of boundary conditions. Mesh size was kept uniform to generate a quasi-ideal mesh following [29] (table S1), which allowed the calculation of average stress values. All models were assigned isotropic material properties for bone ($E = 13.7$ GPa, $\upsilon = 0.3$) and teeth ($E = 38.6$ GPa, $\upsilon = 0.4$) [18]. Only the crowns of the canine teeth were considered in each model, representing the functional unit during initial prey contact.

Two functional scenarios were tested: (i) A non-masticatory bending test to investigate mandibular stability under generalized loading conditions [21]. A single ventrally directed nodal force was applied to the tip of the canine tooth. Load forces were scaled following the quasi-homothetic transformation approach of [30] which ensures correct force/surface area scaling for extruded models as used here. Models were further constrained from movement in x-, y- and z-direction at the jaw joint (three nodes). (ii) A second set of analyses were performed with all

mandibles scaled to the same size and adductor muscle forces applied. Adductor muscle forces were calculated from the size of the attachment area visible in lateral view multiplied by the specific tension (0.3N/mm^2) [31]. All models were further constrained from movement at the tip of the canine tooth (one node in x- and y-direction, but not z-direction to simulate penetration of the prey by the canine).

All models were imported into Abaqus (Simulia, version 6.141) for analysis and post-processing. Biomechanical performance was assessed by per element average von Mises stress (with top 1% of magnitudes values excluded to account for artefacts resulting from point loads) and reaction forces measured at the tip of the canine tooth. Tests for statistical significance of the individual performance metrics were performed in PAST 3.22 [32] (tables S2-4).

(d) Geometric morphometric analysis

To quantify the morphological variation of the analysed taxa, a two-dimensional, landmark-based geometric morphometrics (GMM) approach was used (figure S1*f*). A set of fixed landmarks and semi-landmarks were used to describe the morphology of the skull (8 fixed, 55 semi-landmarks) and the mandible (6 fixed, 25 semi-landmarks) (figure S7), digitised with tpsDig2 [33]. Landmark coordinates were subsequently superimposed using a Procrustes Analysis and then subjected to a Principal Component Analysis (PCA) in PAST 3.22 [32]. PCA scores were used to create morphospace plots (figures S8-10) and to generate performance heatmaps (figure S1*i*) using the R package MBA (https://cran.r-project.org/web/packages/MBA/index.html). Phylomorphospaces were created using the phylogenetic relationships depicted in figure 1.

(e) Phylogeny and evolutionary rates

Time-scaled phylogenetic trees with branch lengths were required to investigate the tempo and mode of biomechanical evolution (figure S1*h*). Tree topologies are composite phylogenies, based on [34,35] for sabre-toothed mammals and [36] for gorgonopsians. The individual sabre-toothed

mammal topologies were combined into a single composite tree for the rates analyses. We use the 'equal' [37] and the fossilized birth–death (FBD) [38,39] time-scaling approaches to test for consistency. Temporal data were based on first appearance dates (FADs) and last appearance dates (LADs), representing the bounds of geological intervals that taxa occurred within. Dating uncertainty was incorporated when time-scaling trees by running 100 iterations and, for each iteration, drawing a single occurrence date for each taxon from a uniform distribution between their FAD and LAD. Traitgrams (phenograms) (figure S11) were generated for each biomechanical character for each subgroup using a randomly selected time-calibrated tree for each group, and maximum-likelihood ancestral state estimation in phytools [40].

Rates of biomechanical evolution were analysed using a Bayesian approach with the variable-rates model in BayesTraits v. 2.0.2 [41]. For the 100 time-scaled iterations of the gorgonopsian tree and the full sabre-toothed mammal tree, rate heterogeneity in each $\log_{10}$ transformed character was tested using a reversible jump Markov Chain Monte Carlo algorithm (rjMCMC). Each tree was run for 200 million iterations, parameters were sampled every 16,000 iterations and the first 40 million iterations were discarded as burn-in. The smallest effective sample size (ESS) was used to assess run convergence. To detect shifts in evolutionary rates, the variable-rates model rescales branches where variance of trait evolution differs from that expected in a homogeneous (Brownian motion) model. The resulting 'rate scalars' represent the amount of evolutionary acceleration or deceleration relative to the background rate along each branch [41,42]. Stepping-stone sampling, with 100 stones each run for 1000 iterations, was used to calculate the marginal likelihood of the models (heterogeneous versus homogeneous rates) [43]. Model fit was compared using Bayes Factors and the Variable Rates Post Processor was used to extract the final parameter values [42]. We summarised rates results for each character by calculating consensus trees from all time-scaled trees that favoured a heterogeneous rates model - giving the mean rate scalars for each branch across gorgonopsians and sabre-toothed mammal phylogeny. Results were consistent in both the 'equal' (figure 4) and FBD dated trees (figure S12).

3. Results

(a) Maximum jaw gape

The biomechanical analyses demonstrate that gape angles vary considerably between species and groups (figure 2*a,* S9*b*). Although there appears to be a trend for the increase (barbourofelids, smilodontines, homotherines) or decrease (nimravids, metailurines) of gape angles through time none of these relationships are statistically significant (table S2). All species across the different lineages show gape angles between 52 and 111 degrees, but diversification patterns differ considerably between groups. Gorgonopsians and nimravids show an "early high disparity" pattern and the widest range of gape values, indicating an early and fast diversification. All other groups exhibit a constant to "late high disparity" trend (figure S12*a*). Effective gape angles (= clearance between upper and lower canines and a proxy for prey size [9]), are considerably lower than the maximum gape angles in all groups (figure 2*a*) but again no statistically significant relationship through time was recovered (table S2). A comparison between actual and effective gape shows a (statistically significant) moderate correlation in homotherines ($R^2 = 0.78$, $p = 6.22E^{-5}$) and nimravids ($R^2 = 0.65$, $p = 0.0009$) but a more decoupled relationship in the other groups ($R^2 = 0.38$-0.63) (table S2, figure S13*a*).

The performance heatmap for the gape angle shows an equal complexity in the evolutionary dynamics. Some (but not all) derived taxa in each group occupy regions of higher performance compared to basal forms (for example in gorgonopsians, barbourofelids, and smilodontines). However, this is not a uniform trend and exceptions are present in each group (figure 3*b*, S14*b*, 15*b*) with derived taxa moving towards low-performance regions. For effective gape angles (figure 3*c*), there is movement between areas of similar performance or towards areas of lower performance than for the basal taxa in each group (figures 3*c,* S14*c*, 15*c)*

Evolutionary rates in jaw gape are heterogeneous for gorgonopsians in the majority of trees analysed (97%). Rapid rates are concentrated in derived rubidgeines, particularly the robustly

214 skulled and large-bodied *Leontosaurus*, *Dinogorgon*, *Rubidgea and Clelandina* (figure 4*a*).
215 *Clelandina* evolved the largest gape angle of all gorgonopsians, whilst *Dinogorgon* and
216 *Leontosaurus* rank amongst the smallest gapes. Similarly, divergent gape angles in closely related
217 taxa are seen in the *Inostrancevia* (large gape) + *Sauroctonus* (small gape) clade – which also
218 exhibit moderately fast rates. In mammalian sabre-toothed taxa, there is mixed evidence for
219 heterogeneous rates, with only 58% of analytical iterations recovering positive evidence for rate
220 variation (figure 4*b*). In these trees, rapid rates are seen in smilodontines (*Megantereon*, *Smilodon*),
221 derived barbourofelids and nimravids (*Pogonodon*, *Hoplophoneus*, *Eusmilus*).
222
223 **(b) Bending strength**
224 Bending strength of the mandible was found to significantly increase with time in barbourofelids
225 and metailurines (figure 2*b*, S16). While nimravids and homotherines also show an increase in
226 bending strength, this trend is not supported statistically. Similarly, the apparent decrease in
227 gorgonopsians and smilodontines is not statistically significant (figure 2*b*, table S2). Bending
228 strength follows a distinct "early high disparity" pattern in nimravids and (to a lesser degree) in
229 gorgonopsians and also smilodontines. All other groups show a "late high disparity" trend (Fig.
230 S9*b*). Overall, bending strength is not correlated with actual gape ($R^2 < 0.2$) and effective gape (R^2
231 < 0.47) (table S3, figure S13*b*, *d*).
232 Similar to gape angle, the evolutionary trends across the performance heatmap show
233 complex movement towards different performance areas (figure 3*d,* S14*d*, S15*d*). As recovered
234 above, only in barbourofelids and metailurines there is a clear trend of derived taxa moving towards
235 high-performance areas.
236 Rates of evolution in bending strength are generally homogeneous for gorgonopsians, with
237 only 20% of iterations showing heterogeneity. In contrast, mammalian sabre-toothed taxa show
238 several bursts of fast evolution in bending strength in 97% of trees. Fast rates are seen in
239 smilodontines and on internal branches uniting metailurines and smilodontines (figure 4*c*). This

reflects both great disparity in smilodontines (e.g. *Smilodon populator* versus *Smilodon fatalis*) and the larger difference between generally high bending resistances in smilodontines compared to low bending strengths in basal metailurines (figure S11*b*). Elsewhere, rapid rates are seen in sister taxa that have divergent bending strengths, notably *Homotherium serum* and *Homotherium venezuelensis*, and the nimravids *Eusmilus* and *Hoplophoneus cerebralis* (figure 4*c*).

(c) Bite force

Barbourofelids and metailurines show a statistically significant trend of decreasing bite forces through time Other groups appear to have a constant (nimravids, homotherines) or increased (gorgonopsians, smilodontines) bite force through time, but these trends are not statistically supported (figures 2*c,* S17, table S2). Gorgonopsians explore a wider range of relative bite forces (ca. 15-35%), while the mammalian sabre-tooths are restricted to lower relative bite forces (ca. 10-25%). No or only weak and statistically not significant correlations were found between bite force and actual gape ($R^2 < 0.04$) and bite force and effective gape ($R^2 < 0.3$), whereas a moderate correlation between bending strength and bite force is observed in barbourofelids ($R^2 = 0.77$, $p = 0.03$) and metailurines ($R^2 = 0.54$, $p = 0.026$) (table S3, figure S13*c, e, f*).

The evolutionary pathways across the performance space show that selected derived taxa in some groups (gorgonopsians, smilodontines) move towards areas of higher performance compared to the basal taxa. However, this trend is not consistent for all derived taxa in these groups. In contrast, barbourofelids and metailurines move towards low-performance areas (figures 3*e,* S14e, S15*e*).

In gorgonopsians, again only 11% of iterations show evidence for rate variation, suggesting that a homogeneous rate (Brownian motion) model is favoured. Accelerated rates of bite force evolution were widely distributed in mammalian sabre-toothed taxa (figure 4*d*) and a heterogeneous rates model is favoured for 94% of analysed trees. Fastest rates are seen in nimravids, particularly *Eusmilus* and *Hoplophoneus*. Other high rate instances involve taxa that evolved contrasting bite

forces compared to their closest relatives. This is seen in homotherines, where *Amphimachairodus* evolved relatively large bite forces, in metailurines, where *Dinofelis* shows notably smaller bite forces than more basal taxa, and in smilodontines, where *Megantereon* has increased bite force relative to others.

4. Discussion

The acquisition of hypertrophied canine teeth and cranial sabre-tooth characteristics across different vertebrate lineages represents a remarkable example of convergent evolution [11]. Despite the close morphological similarities exhibited by individual groups/species, some more general differentiations have been discussed for derived sabre-tooth felids [44,45]: scimitar-toothed cats (i.e. homotherines) with relatively shorter, broad and coarsely-serrated canines and dirk-toothed cats (i.e. smilodontines) with elongate and finely or unserrated canines, each representing a distinct ecomorphology with different cranial functions, as well as differences in their postcranial anatomy [46]. Our new analyses demonstrate that morphofunctional differences and evolutionary dynamics of synapsid sabre-tooths are far more complex. Rather than a clear dichotomous split into two ecomorphologies, we observe a spectrum of functional adaptations. Derived from the combination of the analysed functional parameters (actual and effective gape angle, bending strength, bite force), there are no two clades showing the same distribution of parameters and evolutionary rates (figures 2-4, S14, S15). This confirms assumptions from previous studies on tooth morphology, bite-depth and postcranial specialisations that sabre-tooth function and prey killing strategies evolved along functionally diverse pathways [9,14,18,47]. Discoveries of mosaic-taxa, such a *Xenosmilus hodsonae*, combining scimitar- and dirk-toothed characteristics, had already hinted at the existence of wider morphofunctional diversity [48]. However, it should be noted that only about a fraction of the functional trends through time have been recovered as statistically significant (table S2). This is likely an effect of the divergent functional performances of derived taxa in each group (figure S11) as well as due to the lack of stratigraphic resolution resulting in the same/similar first

appearance dates (in particular for gorgonopsians). In all groups, an increase of functional diversity due to the exploration of different functionspace regions (figure S11) can be observed in the derived taxa which likely dilutes overall trends but lends further proof to the wide diversity of functional adaptations. Consequently, we find no proof for linear functional optimisation of groups as a whole.

Generally, the analyses reveal the emergence of individual species and morphologies with high performances through time but with broad functional diversity and widely distributed high rates leading to functional divergence in each group. For example, an adoption of increased jaw gape and mandibular bending strength is found in most groups, as would be expected following the cranial modifications (i.e. rotation of the braincase, reduction of coronoid process, mental process). While actual gape angles show a range of ca. 60 degrees (reaching up to 111 degrees in *Smilodon fatalis*), effective gape is restricted to a maximum of ca. 70 degrees, with most species ranging between 45 and 65 degrees. This is a similar clearance observed in modern felids [5] and appears to be the most effective gape necessary for prey capture casting further doubt on the idea of all sabre-tooths being large prey specialists [9]. The significant correlation between actual and effective gape in nearly all groups (table S3) suggests that canine length and jaw gape are equally important factors and that canine penetration is more important than maximising prey size [9].

Interestingly, within gorgonopsians, the majority of taxa shows actual gape angles below 80 degrees and effective gape angles below 60 degrees suggesting a possible specialisation towards smaller rather than larger prey, possibly as a strategy to conserve energy expenditure [49]. It is, therefore, possible that the sabre-like canines in gorgonopsians were used to inflict more severe wounds in smaller/similar-sized prey or had an additional function independent of feeding [50,51]. Positioned considerably outside of mammalian synapsids, gorgonopsians were not constrained in their cranial function by a generalised mammalian/carnivoran morphology. In fact, re-modelling of the skull and jaw (e.g. rotation of the facial skeleton, compaction of the braincase, reduction in jaw adductor space, reduction of the coronoid process, increased attachment for post-cranial musculature) is largely absent in gorgonopsians [5]. Furthermore, the gorgonopsian bite technique

318 is significantly dissimilar to that of eutherians: Gorgonopsians used a kinetic-inertial jaw-closing
319 system (analogue to modern crocodilians) relying predominantly on the pterygoideus and
320 temporalis muscle groups to deliver powerful and fast jaw closure [6]. However, the taxa included
321 in our analyses do not account for the entire diversity in gorgonopsian morphology but include
322 mostly larger taxa (e.g. Russian species as well as the morphologically advanced Rubidgeinae [52]).
323 Gorgonopsians only show evolutionary bursts in gape evolution within derived rubidgeines, but bite
324 force and bending strength evolved following a homogeneous rates model. This result may, in part,
325 be due to a low sample size for this group and failure to detect rate variation.
326 While there appears to be a trend towards increased relative bite forces in gorgonopsians and
327 smilodontines, only the decrease of relative bite force through time in barbourofelids and
328 metailurines is statistically supported. This seemingly counterintuitive trend in barbourofelids may
329 be explained with the increasing specialisation and evolution of a novel prey killing strategy in
330 derived taxa. With a shift from a killing bite (similar to modern felids) powered by the jaw muscles,
331 to a canine-shear bite harnessing the neck musculature [45, 47, 53] bite-force becomes less
332 important. At the same time, the emphasis on large jaw gape and canine clearance requires a
333 reorganisation of the jaw adductor musculature changing the mechanical advantage and therefore
334 constraining the ability to produce high bite forces [4,5,13].
335 The canine-shear bite has also been accepted as the main killing mode in *Smilodon fatalis*
336 and other smilodontines [3,13]. However, while derived smilodontines have among the highest
337 actual gape angles, bite forces are not decreasing through time as in barbourofelids. This may be
338 because relative bite forces are within a similar range in derived smilodontines (ca. 15-20 degrees)
339 to those in derived barbourofelids (ca. 12-17 degrees). A canine-shear bite is therefore likely to be
340 the main killing style in both groups. However, the lower bending strength of the mandible in
341 derived smilodontines would have, in contrast to barbourofelids with their prominently developed
342 mental processes, required more powerful forelimbs to restrain prey [8,10,47]. Metailurines parallel
343 barbourofelids closely in increasing mandibular bending strength and decreasing relative bite forces

through time. However, metailurines do not show the extent of cranial and mandibular modifications indicative of a canine-shear bite. It is, therefore, possible, that these trends reflect an adaptation to small prey in derived metailurines. In contrast, homotherines would have engaged in a different killing technique as indicated by moderate values and no significant changes through time of all functional parameters. Homotherines likely employed a predatory behaviour between a clamp-and-hold bite (analogue to modern pantherines) and a canine-shear bite as suggested by previous morphological and biomechanical analyses [18,48]. Nimravids generally show high jaw gapes (i.e. majority of taxa with actual gape angles over 90 degrees) and bending strength values with little change through time. This could represent an intermediate killing strategy for nimravids (as previously hypothesised based on the analysis of mandibular force profiles) [10] with a specialisation towards large-bodied prey [47] for which large gape angles and bending strength would be necessary.

The evolutionary pathways across the performance heatmaps (figure 3) further support the hypothesis that the different sabre-tooth species and groups pursued different hunting/killing strategies. However, they also show that there is no single consistent trend towards functional optimisation as hypothesised in the past [11]. All analysed groups span a wide range between basal and derived members across the heatmaps/morphospace. With the exception of metailurines, which are restricted to small areas of the mandibular, cranial and combined morphospaces, all groups can be found expanding into different regions of the morphospace (figures 3*a*, S14*a*, S15*a*). Anatomically, this represents an adoption of "typical sabre-tooth" morphologies (i.e. anteroposteriorly short but dorsoventrally high skulls, a reduced coronoid process, an expanded mental process) towards one end and the retention of "cat-like" morphologies (i.e. relatively shorter canines, low braincase, high coronoid process) on the other end (figures 3*a*, S14*a*, S15*a*). Again, gorgonopsians form the exception in occupying mostly distinct areas in the morphospace, with only occasional intrusions into the areas occupied by the mammalian taxa (figures 3a, S15*a*). This

pattern further supports the assumption that felid sabre-tooths were highly specialised but morphofunctionally constrained, possibly due to a high degree of functional integration [35].

It is further noteworthy that metailurines, homotherines and smilodontines show different or even opposing functional performances and that divergent functional morphologies are linked to rapid evolutionary shifts in some derived taxa in each group (figure 4). These three groups had considerable spatial and temporal overlap with several sabre-tooth species sharing the same ecosystem with each other and other mammalian carnivores [54,55]. Fast rates and different functional performances, therefore, suggest selective pressures, considerable specialisation and niche-partitioning to avoid intra- and interclade competition. Our results parallel previous findings that mandible shape in sabre-toothed cats evolved at a higher rate than in modern conical toothed cats [34]. This demonstrates that although a large degree of morphological convergence is present in these groups, functional characteristics are much more variable and diverse.

References

1. Werdelin, L., McDonald, H. G., & Shaw, C. A. *Smilodon: The Iconic Sabretooth*. (JHU Press, 2018).
2. Warren, J. C. Remarks on *Felis Smylodon*. *Proceedings of the Boston Society of Natural History*. IV, 256–258 (1853).
3. Akersten, W.A. Canine function in *Smilodon* (Mammalia; Felidae; Machairodontinae). *Contributions to Science of the Natural History Museum Los Angeles.* **356**, 1–22 (1985).
4. McHenry, C.R., Wroe, S., Clausen, P.D., Moreno, K. & Cunningham, E. Supermodeled sabrecat, predatory behavior in *Smilodon fatalis* revealed by high-resolution 3D computer simulation. *Proceedings of the National Academy for Science*. **104**, 16010–16015 (2007).
5. Emerson, S. B. & Radinsky, L. B. Functional analysis of sabretooth cranial morphology. *Paleobiology*. **6**, 295–312 (1980).
6. Van Valkenburgh, B. & Jenkins, I. Evolutionary patterns in the history of Permo-Triassic and Cenozoic synapsid predators. *Paleontological Society Papers*. **8**, 267–288 (2002).
7. Christiansen, P. Phylogeny of the sabretoothed felids (Carnivora: Felidae: Machairodontinae). *Cladistics*, **29**, 543-559 (2013).
8. Meachen-Samuels, J. A. & Van Valkenburgh, B. Radiographs reveal exceptional forelimb strength in the sabretooth cat, *Smilodon fatalis*. *PLoS One*, **5**, e11412 (2010).
9. Andersson, K., Norman, D. & Werdelin, L. Sabretoothed carnivores and the killing of large prey. *PLoS One*, **6**, e24971 (2011).
10. Therrien, F. Feeding behaviour and bite force of sabretoothed predators. *Zoological Journal of the Linnean Society*, **145**, 393-426 (2005).
11. Van Valkenburgh, B. Déjà vu: the evolution of feeding morphologies in the Carnivora. *Integrative and Comparative Biology*, **47**, 147-163 (2007).
12. Antón, M., & Galobart, À. Neck function and predatory behavior in the scimitar toothed cat *Homotherium latidens* (Owen). *Journal of Vertebrate Paleontology*, **19**, 771-784 (1999).

13. Christiansen, P. Comparative bite forces and canine bending strength in feline and sabretooth felids: implications for predatory ecology. *Zoological Journal of the Linnean Society*, **151**, 423-437 (2007).
14. Slater, G. J., & Van Valkenburgh, B. Long in the tooth: evolution of sabretooth cat cranial shape. *Paleobiology*, **34**, 403-419 (2008).
15. Losos, J. B. Convergence, adaptation, and constraint. *Evolution*, **65**, 1827-1840 (2011)
16. Lautenschlager, S., Brassey, C. A., Button, D. J., & Barrett, P. M. Decoupled form and function in disparate herbivorous dinosaur clades. *Scientific Reports*, **6**, 26495 (2016).
17. Figueirido, B., MacLeod, N., Krieger, J., De Renzi, M., Pérez-Claros, J. A., & Palmqvist, P. Constraint and adaptation in the evolution of carnivoran skull shape. *Paleobiology*, **37**, 490-518 (2011).
18. Figueirido, B., Lautenschlager, S., Pérez-Ramos, A., & Van Valkenburgh, B. Distinct Predatory Behaviors in Scimitar-and Dirk-Toothed Sabretooth Cats. *Current Biology*, **28**, 3260-3266 (2018).
19. Pierce, S. E., Angielczyk, K. D., & Rayfield, E. J. Patterns of morphospace occupation and mechanical performance in extant crocodilian skulls: a combined geometric morphometric and finite element modeling approach. *Journal of Morphology*, **269**, 840-864 (2008).
20. Polly, P. D., Stayton, C. T., Dumont, E. R., Pierce, S. E., Rayfield, E. J., & Angielczyk, K. D. Combining geometric morphometrics and finite element analysis with evolutionary modeling: towards a synthesis. *Journal of Vertebrate Paleontology*, **36**, e1111225 (2016).
21. Tseng, Z. J., & Flynn, J. J. Structure-function covariation with nonfeeding ecological variables influences evolution of feeding specialization in Carnivora. *Science Advances*, **4**, eaao5441 (2018).
22. Rahman, I. A., & Lautenschlager, S. Applications of three-dimensional box modeling to paleontological functional analysis. *The Paleontological Society Papers*, **22**, 119-132 (2016).

433 23. Morales-García, N. M., Burgess, T. D., Hill, J. J., Gill, P. G. & Rayfield, E. J. The use of
434 extruded finite-element models as a novel alternative to tomography-based models: a case
435 study using early mammal jaws. *Journal of the Royal Society Interface*, **16**, 20190674
436 (2019).
437 24. Lautenschlager, S. Estimating cranial musculoskeletal constraints in theropod dinosaurs.
438 *Royal Society Open Science*, **2**, 150495 (2015).
439 25. Fletcher, T. M., Janis, C. M., & Rayfield, E. J. Finite element analysis of ungulate jaws: can
440 mode of digestive physiology be determined. Palaeontologia Electronica, **13**, 1-15 (2010).
441 26. Young, M. T., Brusatte, S. L., Ruta, M. & de Andrade, M. B. The evolution of
442 Metriorhynchoidea (Mesoeucrocodylia, Thalattosuchia): an integrated approach using
443 geometric morphometrics, analysis of disparity, and biomechanics. *Zoological Journal of*
444 *the Linnean Society*, **158**, 801-859 (2010).
445 27. Neenan, J. M., Ruta, M., Clack, J. A. & Rayfield, E. J. Feeding biomechanics in
446 Acanthostega and across the fish–tetrapod transition. *Proceedings of the Royal Society B:*
447 *Biological Sciences*, **281**, 20132689 (2014).
448 28. Serrano-Fochs, S., De Esteban-Trivigno, S., Marcé-Nogué, J., Fortuny, J., Fariña, R.A..
449 Finite Element Analysis of the Cingulata Jaw: An Ecomorphological Approach to
450 Armadillo's Diets. PLoS One **10**, e0120653 (2015).
451 29. Marcé Nogué, J., de Esteban-Trivigno, S., Escrig Pérez, C. & Gil Espert, L. Accounting for
452 differences in element size and homogeneity when comparing Finite Element models:
453 Armadillos as a case study. *Palaeontologia Electronica*, **19**, 1-22 (2016).
454 30. Marcé-Nogué, J., DeMiguel, D., Fortuny, J., de Esteban-Trivigno, S., Gil, L. Quasi-
455 homothetic transformation for comparing the mechanical performance of planar models in
456 biological research. *Palaeontologia Electronica*, **16**, 1-15 (2013).

457 31. Thomason, J. J., Russell, A. P., & Morgeli, M. Forces of biting, body size, and masticatory
458 muscle tension in the opossum *Didelphis virginiana*. *Canadian Journal of Zoology*, **68**, 318-
459 324 (1990).
460 32. Hammer, Ø., Harper, D. A. & Ryan, P. D. PAST: paleontological statistics software package
461 for education and data analysis. *Palaeontologia Electronica*, **4**, 1-9 (2001).
462 33. Rohlf, F.J. TpsDig 2. (Department of Ecology and Evolution. State University of New York,
463 Stony Brook, NY, 2010)
464 34. Piras, P., Silvestro, D., Carotenuto, F., Castiglione, S., Kotsakis, A., Maiorino, L.,
465 Melchionna, M., Mondanaro, A., Sansalone, G., Serio, C. & Vero, V. A. Evolution of the
466 sabretooth mandible: A deadly ecomorphological specialization.
467 35. Piras, P., Maiorino, L., Teresi, L., Meloro, C., Lucci, F., Kotsakis, T., & Raia, P. Bite of the
468 cats: relationships between functional integration and mechanical performance as revealed
469 by mandible geometry. *Systematic Biology*, **62**, 878-900 (2013).
470 36. Bendel, E. M., Kammerer, C. F., Kardjilov, N., Fernandez, V. & Fröbisch, J. Cranial
471 anatomy of the gorgonopsian *Cynariops robustus* based on CT-reconstruction. *PloS one*, **13**,
472 e0207367 (2018).
473 37. Brusatte, S. L., Benton, M. J., Ruta, M. & Lloyd, G. T. Superiority, Competition, and
474 Opportunism in the Evolutionary Radiation of Dinosaurs. *Science*, **321**, 1485-91488 (2008).
475 38. Zhang, C., Stadler, T., Klopfstein, S., Heath, T. A., & Ronquist, F. Total-evidence dating
476 under the fossilized birth–death process. *Systematic Biology*, **65**, 228–249 (2015).
477 39. Matzke, N. J., & Wright, A. Inferring node dates from tip dates in fossil Canidae: the
478 importance of tree priors. *Biology Letters*, **12**, 20160328 (2016).
479 40. Revell, L. J. Phytools: an R package for phylogenetic comparative biology (and other
480 things). *Methods in Ecology and Evolution* **3**, 217-223 (2012).
481 41. Venditti, C., Meade, A. & Pagel, M. Multiple routes to mammalian diversity. *Nature* **479**,
482 393-396 (2011).

42. Baker, J., Meade, A., Pagel, M. & Venditti, C. Positive phenotypic selection inferred from phylogenies. *Biological Journal of the Linnean Society.* **118**, 95-115 (2016).

43. Xie, W., Lewis, P. O., Fan, Y., Kuo, L., & Chen, M. H. Improving marginal likelihood estimation for Bayesian phylogenetic model selection. *Systematic Biology*, **60**, 150-160 (2011).

44. Kurten, B. *Pleistocene mammals of Europe*. (Routledge Press, 1968).

45. Martin, L. D. Functional morphology and the evolution of cats. *Transactions of the Nebraska Academy of Sciences*, **8**, 141-154 (1980).

46. Anyonge, W. Locomotor behaviour in Plio-Pleistocene sabre-tooth cats: a biomechanical analysis. *Journal of Zoology*, **238**, 395-413 (1996).

47. Meachen-Samuels, J. A. Morphological convergence of the prey-killing arsenal of sabretooth predators. *Paleobiology*, **38**, 1-14 (2012).

48. Martin, L. D., Babiarz, J. P., Naples, V. L. & Hearst, J. Three ways to be a sabre-toothed cat. *Naturwissenschaften*, **87**, 41-44 (2000).

49. Carbone, C. Teacher, A., & Rowcliffe, J. M. The costs of carnivory. *PLoS Biology*, **5,** 1-6 (2007).

50. Benoit, J., Manger, P. R., Fernandez, V. & Rubidge, B. S. Cranial bosses of *Choerosaurus dejageri* (Therapsida, Therocephalia): earliest evidence of cranial display structures in eutheriodonts. *PloS One*, **11**, e22 (2016).

51. Kammerer, C. F. Systematics of the Rubidgeinae (Therapsida: Gorgonopsia). *PeerJ*, **4**, e1608 (2016).

52. Kammerer, C. F. & Masyutin, V. Gorgonopsian therapsids *(Nochnitsa* gen. nov. and *Viatkogorgon*) from the Permian Kotelnich locality of Russia. *PeerJ*. **6**, e4954 (2018).

53. Martin, L. D., Schultz, C. B. & Schultz, M. R. Sabre-toothed cats from the Plio-Pleistocene of *Nebraska. Transactions of the Nebraska Academy of Sciences,* **16**, 153-163 (1988).

54. Hunt Jr, R. M. Biogeography of the order Carnivora. *Carnivore behavior, ecology, and evolution*, ***2***, 485-541 (1996).

55. Van Valkenburgh, B. Major patterns in the history of carnivorous mammals. *Annual Review of Earth and Planetary Sciences*, **27**, 463-493 (1999).

Data accessibility. All data files are available via the following link: https://beardatashare.bham.ac.uk/getlink/fiR7wvK357hbPrQ9FVg6eR1Q/ Upon acceptance the files will be moved to a permanent repository (e.g. Dryad).

Authors' contributions. S.L conceived the study and designed the analyses. S.L., D.D.C and T.L.S. conducted the analyses and designed the figures. B.F and E.-M.B. contributed to the datasets. All authors contributed to the writing of the manuscript.

Competing interests. We declare we have no competing interests.

Funding. T.L.S. was funded by ERC grant 788203 (INNOVATION). B.F. was funded by the Spanish Ministry of Science and Competitiveness (Grants CGL2015-68300P; CGL2017-92166-EXP).

Acknowledgements. The authors are very grateful to Armin Elsler (University of Bristol) for sharing R code that aids the processing and plotting of outputs from BayesTraits. Part of this work was carried out using the computational facilities of the Advanced Computing Research Centre, University of Bristol. Jordi Marcé-Nogue and Robert Brocklehurst are thanked for constructive suggestions improving the manuscript.

530 **Figure captions**

531 **Figure 1:** Sabre-toothed vertebrates in their phylogenetic context. Taxa are represented by skull
532 outlines with the mandible opened at the maximum gape angle. Composite phylogenetic tree based
533 on [34-36].
534

535 **Figure 2:** Biomechanical performance for different sabre-toothed clades through time: (*a*) actual
536 (solid lines) and effective (dotted lines) gape angle; (*b*) average bending strength of the mandible
537 tested in non-masticatory scenario; (*c*) relative bite force (bite efficiency) based on ratio between
538 absolute bite forces and muscle forces.
539

540 **Figure 3:** Morphospace and performance space occupation of studied sabre-tooth species (crania
541 and mandibles combined): (*a*) morphospace with convex hulls for different groups obtained from
542 the Procrustes coordinates of the landmark analysis; (*b*) performance heatmap with actual gape
543 angle values plotted onto morphospace; (*c*) performance heatmap with effective gape angle values
544 plotted onto morphospace; (*d*) performance heatmap with bending strength values plotted onto
545 morphospace; (*e*) performance heatmap with bite force values plotted onto morphospace.
546 Phylogenetic relationships as in fig. 1 superimposed on heatmaps.
547

548 **Figure 4:** Rates of biomechanical evolution in sabre-toothed vertebrates: *(a)* rates of evolution in
549 gorgonopsian gape angle summarised from 97 heterogeneous rate trees; *(b)* evolutionary rates in
550 sabre-toothed mammal gape angle showing the consensus tree from 58 heterogeneous rate trees; *(c)*
551 rates of evolution in sabre-toothed mammal bending strength summarised from 97 heterogeneous
552 rate trees; *(d)* evolutionary rates in sabre-toothed mammal bite force illustrating consensus results
553 from 94 heterogeneous rate trees. Rates of evolution in gorgonopsian bending strength and bite
554 force were homogeneous. In each plot, phylogenetic branches and tip labels are coloured according
555 to evolutionary rates, grading from slow to fast as denoted by the keys. The branch lengths are
556 scaled to time and based on the average lengths from the time-scaled input trees. Results were
557 consistent in both the 'equal' and FBD dated trees (figure S12).

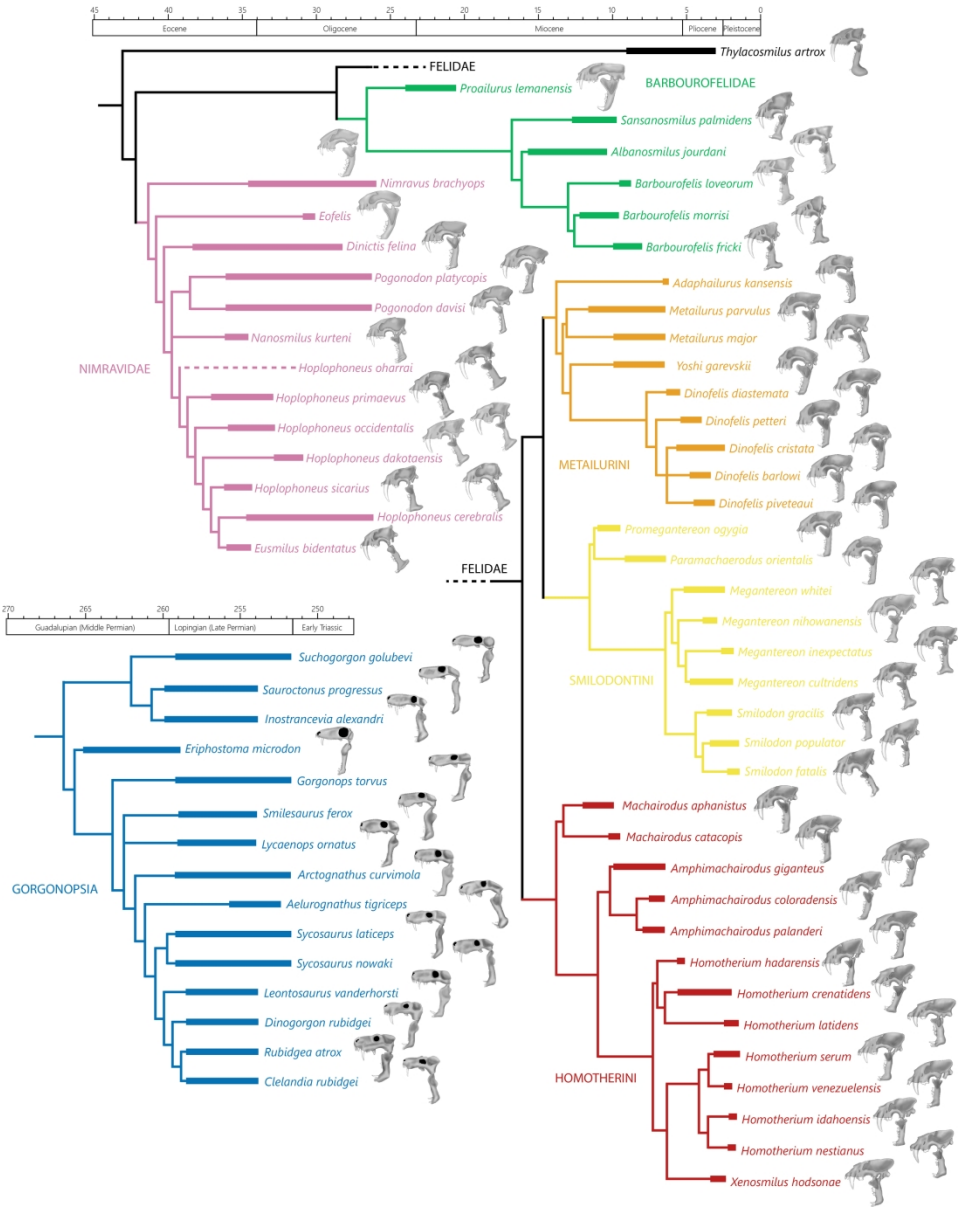

Figure 1: Sabre-toothed vertebrates in their phylogenetic context. Taxa are represented by skull outlines with the mandible opened at the maximum gape angle. Composite phylogenetic tree based on [34-36].

209x262mm (300 x 300 DPI)

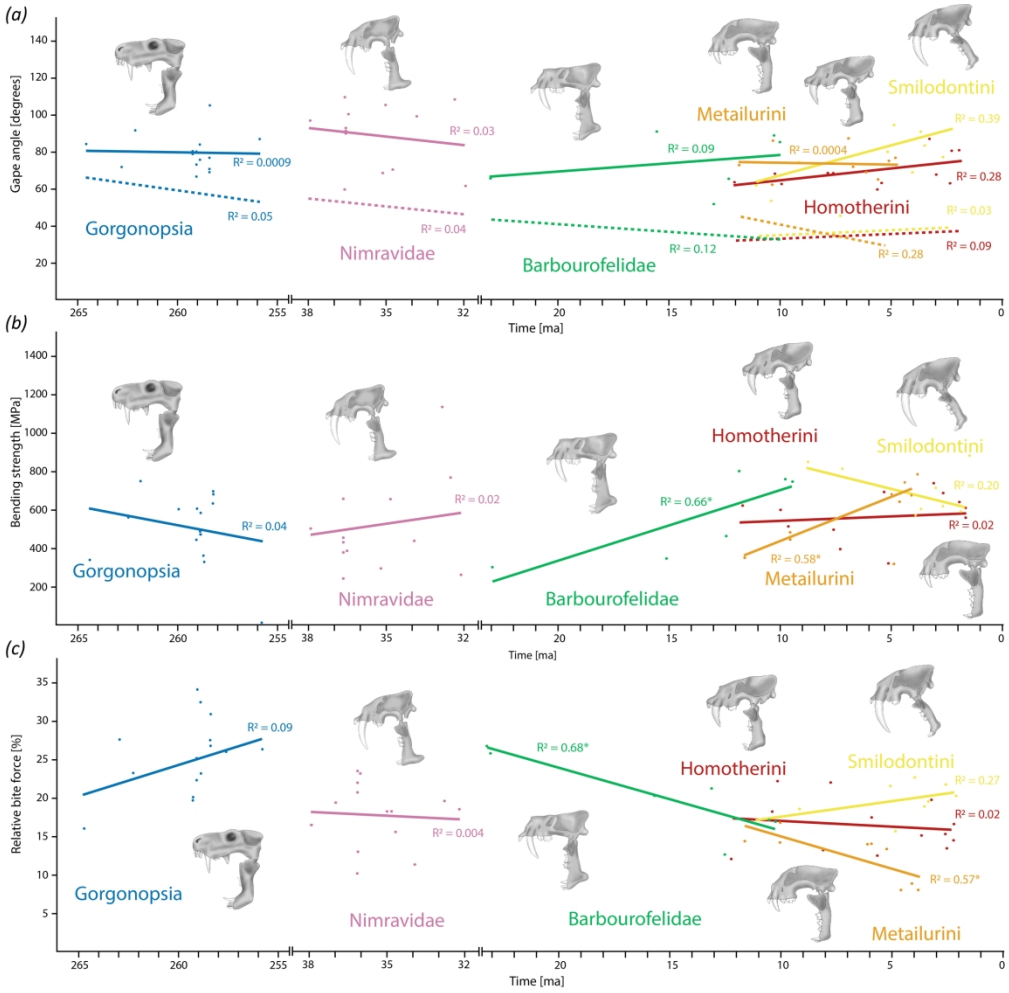

Figure 2: Biomechanical performance for different sabre-toothed clades through time: (a) actual (solid lines) and effective (dotted lines) gape angle; (b) average bending strength of the mandible tested in non-masticatory scenario; (c) relative bite force (bite efficiency) based on ratio between absolute bite forces and muscle forces.

212x208mm (300 x 300 DPI)

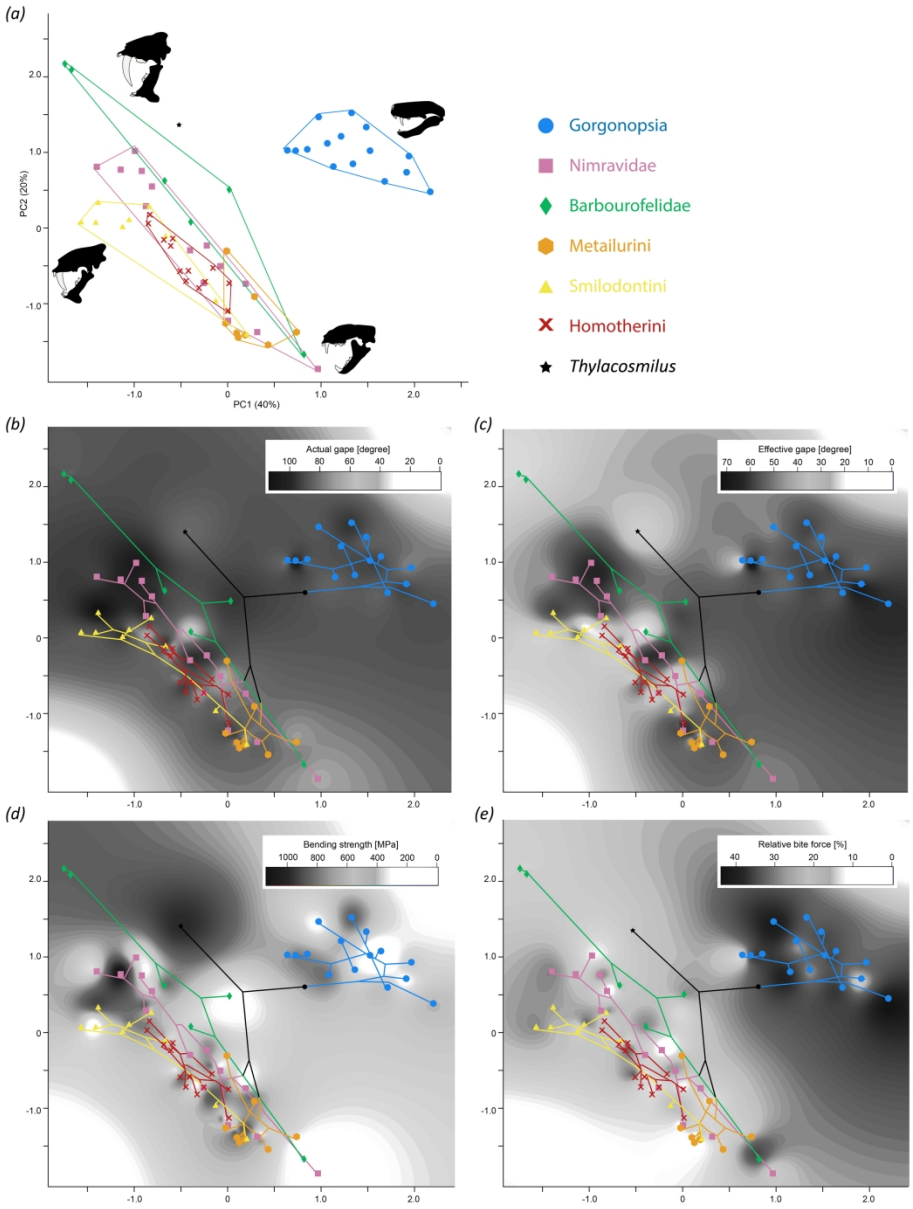

Figure 3: Morphospace and performance space occupation of studied sabre-tooth species (crania and mandibles combined): (a) morphospace with convex hulls for different groups obtained from the Procrustes coordinates of the landmark analysis; (b) performance heatmap with actual gape angle values plotted onto morphospace; (c) performance heatmap with effective gape angle values plotted onto morphospace; (d) performance heatmap with bending strength values plotted onto morphospace; (e) performance heatmap with bite force values plotted onto morphospace. Phylogenetic relationships as in fig. 1 superimposed on heatmaps.

211x279mm (300 x 300 DPI)

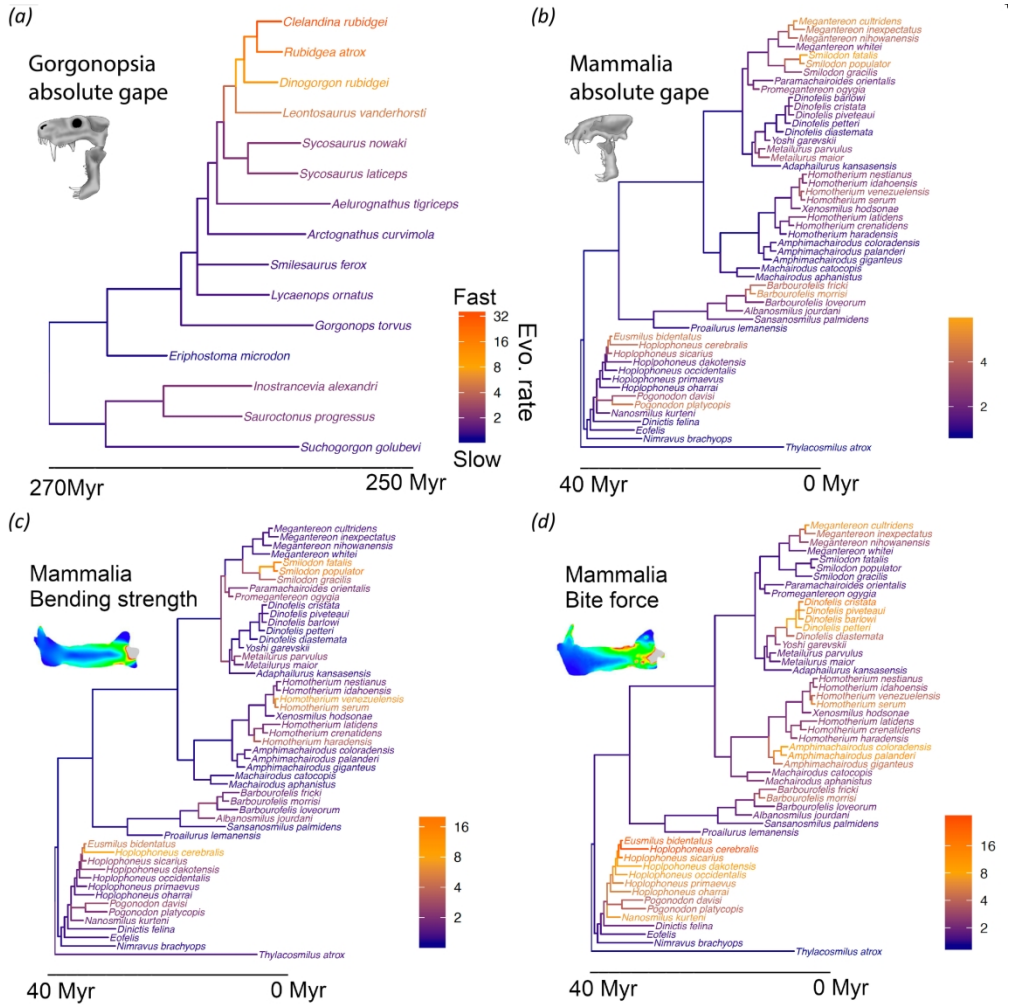

Figure 4: Rates of biomechanical evolution in sabre-toothed vertebrates: (a) rates of evolution in gorgonopsian gape angle summarised from 97 heterogeneous rate trees; (b) evolutionary rates in sabre-toothed mammal gape angle showing the consensus tree from 58 heterogeneous rate trees; (c) rates of evolution in sabre-toothed mammal bending strength summarised from 97 heterogeneous rate trees; (d) evolutionary rates in sabre-toothed mammal bite force illustrating consensus results from 94 heterogeneous rate trees. Rates of evolution in gorgonopsian bending strength and bite force were homogeneous. In each plot, phylogenetic branches and tip labels are coloured according to evolutionary rates, grading from slow to fast as denoted by the keys. The branch lengths are scaled to time and based on the average lengths from the time-scaled input trees. Results were consistent in both the 'equal' and FBD dated trees (figure S12).

209x209mm (300 x 300 DPI)